# Exhibit 4

Ultrastructural Pathology

ISSN: 0191-3123 (Print) 1521-0758 (Online) Journal homepage: https://www.tandfonline.com/loi/iusp20

# Magnesium/silicon atomic weight percent ratio standards for the tissue identification of talc by scanning electron microscopy and energy dispersive X-ray analysis

Sandra A. McDonald, Yuwei Fan, Rick A. Rogers & John J. Godleski

**To cite this article:** Sandra A. McDonald, Yuwei Fan, Rick A. Rogers & John J. Godleski (2019): Magnesium/silicon atomic weight percent ratio standards for the tissue identification of talc by scanning electron microscopy and energy dispersive X-ray analysis, Ultrastructural Pathology, DOI: 10.1080/01913123.2019.1692119

**To link to this article:** https://doi.org/10.1080/01913123.2019.1692119

Published online: 16 Nov 2019.

ULTRASTRUCTURAL PATHOLOGY
https://doi.org/10.1080/01913123.2019.1692119

Taylor & Francis
Taylor & Francis Group



# Magnesium/silicon atomic weight percent ratio standards for the tissue identification of talc by scanning electron microscopy and energy dispersive X-ray analysis

Sandra A. McDonald[a], Yuwei Fan[a,b,c], Rick A. Rogers[d,e], and John J. Godleski[a,e,f]

[a]John J. Godleski, MD PLLC, Milton, MA, USA; [b]Electron Microscopy Laboratory, Department of Environmental Health, Harvard TH Chan School of Public Health, Boston, MA, USA; [c]Boston University School of Dental Medicine, Boston, MA, USA; [d]Rogers Imaging Corporation, Natick, MA, USA; [e]Department of Environmental Health, Harvard TH Chan School of Public Health, Boston, MA, USA; [f]Pathology Emeritus, Harvard Medical School, Boston, MA, USA

**ABSTRACT**

Talc may lodge in human tissues through various routes, and has been associated with the development of ovarian carcinoma in case control epidemiologic studies. Talc is detected in tissues with scanning electron microscopy and energy dispersive X-ray analysis (SEM/EDS), with expected magnesium (Mg) and silicon (Si) peaks. The theoretical atomic weight % Mg/Si ratio for talc is 0.649, and for diagnostic purposes, a range of ± 5% (~0.617 to 0.681) is often used as a standard. Our goal was to establish empirically the quantitative range for talc identification by SEM/EDS using two source materials: a Johnson's Baby Powder™ (cosmetic-grade) consumer sample, and talc from Sigma-Aldrich (particle-grade material intended for scientific use). We examined 401 Mg-Si particles with SEM/EDS across the two samples, using two different SEM microscopes. Overall, we found a mean Mg/Si atomic weight % ratio of 0.645, with minimal differences between study subsets. The standard deviation was 0.025; (± 1σ = 0.620–0.670). The currently used ± 5% diagnostic range (Mg/Si 0.617–0.681) is thus reasonably close to this study's ± 1σ range, and well within a ± 2 σ confidence interval span (Mg/Si 0.595–0.695). The ± 5% range is thus an appropriately conservative standard whose continued use seems justified.

**ARTICLE HISTORY**
Received 30 October 2019
Accepted 8 November 2019

**KEYWORDS**
Phrases: talc; scanning electron microscopy; energy dispersive X-ray spectroscopy; diagnosis; pathology

## Introduction

Talc is a stable, crystalline, magnesium-containing sheet silicate (a member of a class of phyllosilicates), chemical formula $Mg_3Si_4O_{10}(OH)_2$, which is found in the earth's crust and mined in varied parts of the world. It is a broadly used and frequently encountered substance in cosmetics, manufacturing, construction, and other industries[1] that may lodge in human tissues through several means: inhalation, injection, use in medical procedures (pleurodesis), and topical application to the perineum. In the latter setting, it has been used as a consumer product to lubricate skin, absorb excess moisture, and promote overall hygiene and comfort. Currently, there is medical, public health, and medicolegal interest in the association of ovarian cancers with the use of talc-containing products in the genital area. This association has been supported by various epidemiologic studies which found a clear excess of women with ovarian malignancy who had used talc in that location beforehand, compared to control women[2–6], with an overall risk ratio of around 1.3.[7] The International Agency for Research on Cancer has declared the use of talc (not containing asbestos) in the genital area as possibly carcinogenic (Class 2B).[8] Recently, the demonstration through laboratory and spectroscopic means that talc is present in the ovarian tissue and/or genital tract from talc-exposed women with ovarian cancer has been of increased importance, both in morphology-based studies and in specific patients with ovarian carcinoma in the medicolegal setting.[9–11] Analysis in the latter situation helps to establish past or present exposure in a given patient, and provides evidence for the epidemiologic association within a specific case. Talc in the genital tract of women is thought to migrate there from the initial exposure site in the

**CONTACT** Sandra A. McDonald sandram8690@gmail.com work: 304 Central Ave., Milton, MA 02186; Home: Apartment 1714, 175Q Centre Street, Quincy, MA 02169, USA

Color versions of one or more of the figures in the article can be found online at www.tandfonline.com/iusp.

perineum, from where it may either undergo direct upward transport through the tract, or gain access to lymphatics with subsequent lodging in various lymphvascular-rich pelvic organs and sites.[10]

The identification of talc in human tissues is an important example of how the diagnosis and quantification of foreign material in tissue is needed to document exposure, and to correlate with disease occurrence or severity related to that tissue.[12] This concept is perhaps best known for asbestos and pleural mesothelioma and pulmonary fibrosis.[13] For all tissue-based methods, transmission electron microscopy (TEM) or scanning electron microscopy (SEM) and energy dispersive x-ray spectroscopy (EDS) are used to find exogenous particles, and verify that their elemental signatures are consistent with a specific type of foreign material exposure[14], including medicolegal contexts where there are claims of injury from such exposures.[12] SEM with EDS often is the most useful and practical quantitative instrument available for the detection of exogenous material in paraffin-embedded human tissue[14], and is the one we use for talc diagnosis. The most comprehensive quantification is obtained by digestion of a tissue sample, which uses much larger amounts of tissue than can be assessed in a histologic tissue section[12], but this method is susceptible to contamination issues, requires the destruction of sample, and causes anatomic landmarks to be lost.[9] A better, nondestructive method for the detection of talc in paraffin tissue blocks (the most common type of specimen that becomes available in medicolegal cases) is correlative polarizing light microscopy and *in situ* SEM/EDS (a method originally described by Thakral and Abraham.[15]) This method utilizes the birefringence of talc, and the preservation of architectural information in light microscopy followed by *in situ* SEM/EDS, to correlatively assess the quantity and location of talc particles in the paraffin-embedded tissue. In this method, the paraffin tissue block is inserted directly into the SEM chamber under variable pressure (i.e. partial vacuum), and the incident electron beam applied to the tissue-containing surface of the carbonaceous block. Under the SEM conditions we typically use, the penetration depth of the beam is estimated to be 2.5 μm (principles of electron-specimen interactions and specimen depth reviewed by Goldstein et al.[16])

Talc has a three-layer sheet structure with a positively charged magnesium-containing octahedral layer between two negatively charged tetrahedral silicate layers. Talc sheets are bound to each other by relatively weak van der Walls forces, allowing them to slide and glide over each other easily[17], thus giving talc both its status as the softest known mineral, and its tendency to be in the form of platy particles under microscopic examination. In fact, in both commercial samples and tissue sections, talc may morphologically appear as plates, polygons and fibrous forms, a fiber being defined as an elongated structure having an aspect ratio of 3:1 or greater[18] and approximately parallel sides.[12,14] The platy particles are often isodiametric (i.e. length and width not widely disparate) but they may mimic fibers when viewed on edge. When present, talc is readily visible in histologic tissue sections under polarizing light microscopy, where it is brightly birefringent.

Identification of talc by SEM/EDS begins with its strong positivity under backscattered electron imaging (BEI), a technique where beam electrons are elastically deflected more than 90 degrees from their forward motion, and detected based on (among several possible modes) the presence of high atomic number elements in a sample.[19] EDS spectral analysis of talc particles (using a spot quantitative mode) yields magnesium, oxygen and silicon peaks. Traces (EDS atomic weight % of <2%) of other elements such as Al, Ca, Na, K, and Fe may occasionally be present, given that small impurities may be present within mined talc, arise during manufacture processing, or contaminate talc samples at a subsequent stage. However, based on talc's chemical formula, especially the stoichiometry of three Mg atoms to every four Si atoms, pure talc has a theoretical Mg/Si atomic ratio of 0.750 and atomic weight % ratio of 0.649.

Using standard materials or "standardless analyses"[20], variation in the quantitative measurements of any particle can be expected, depending on the purity of the substance, as well as factors associated with the analytical methodology. The detection of element-specific X-ray signals in EDS relies on a sequence of interactions between incident electrons and electron orbital energy

levels that contain inherent imprecisions that produce some natural variation in measured chemical parameters. Some of these vary across systems. Some apply to the differential between the weaker kiloelectron volt (keV) X-ray signals for magnesium compared with silicon. For example, a talc particle located relatively deep within paraffin tissue and studied with the SEM/EDS *in situ* method[15] may require a longer distance for emitted X-ray signals to escape and reach the detector, and this could unpredictably enhance the differential between the weaker-energy Mg signals and the stronger Si signals. Another consideration is that in EDS spectrum samples, only a small proportion of the total atoms in a sample are analyzed. Simple stoichiometric, density and atomic weight calculations show that in a typical 1 μm talc particle (approximated as a 1 $\mu m^3$ volume), there are ~1.4E10 Mg atoms and ~1.9E10 Si atoms; the comparable figures for a 5 μm talc particle are ~1.8E12 Mg atoms and ~2.3E12 Si atoms. For a typical EDS run involving 5000 counts per second and a 30-second collection time, about 150,000 atoms are assessed, or roughly one in every $10^8$ atoms in a 5 μm particle (exclusive of oxygen). Also, electron beam analysis for talc particles in tissue or on the surface may study only a fraction of the mass, since penetration depth is limited to ~1 μm in talc, based on a Monte Carlo algorithm for the scattering of penetrating electrons within solids.[21,22]

Therefore, considering all of these factors, a margin of ±5% for the Mg/Si atomic weight percent ratio (approximately 0.617 to 0.681) has been used in human tissue diagnosis[9,10] (along with the expected clinical/historical information and morphologic features) to assure that the detected material is talc. This ±5% range has support in the literature as a generally appropriate EDS standard based on a broad variety of chemical constituents and analyses.[20] We undertook this study to show that the ±5% range applies well to talc specifically, based on empiric evidence gathered from the analysis of two different commercially available talc samples, using SEM microscopes from two different manufacturers, each one having an EDS detector from the same manufacturer, but which were physically separate instruments. We measured the statistical distribution of Mg/Si atomic weight % ratios in a representative large group of talc particles in the samples, and compared those to the currently used diagnostic range. We were particularly interested in how the ± 5% range for talc compared to the ±1σ and ±2σ standard deviation thresholds in the commercial samples.

## Materials and methods

A 4 oz bottle of Johnson's Baby Powder™ (JBP) (lot number 8137–003011, Johnson and Johnson Consumer Companies, Skillman, NJ) was purchased over-the-counter from a local retail pharmacy in 2012, and subsequently kept sealed under airtight conditions and protected from heat, light, and other environmental factors. The ingredient list for JBP listed talc and fragrance as the contents of the container. Two small samples of JBP were taken from the bottle with a small flame-cleaned stainless steel spatula, and a thin coating of talc (appropriately low particle density) applied to separate 12 mm-diameter carbon discs with double-sided adhesive (Cat#775825-12, Electron Microscopy Sciences, Hatfield, PA); these discs were in turn mounted on similarly-sized circular aluminum stubs. Excess JBP material was removed from the disc surfaces prior to SEM analysis. A separate carbon disc of the same type but without JBP was also mounted for control purposes, as was a bare aluminum stub (i.e. without either talc powder sample or a carbon disc).

The four stubs (i.e. two JBP samples, one carbon disc blank control, and one metal stub control) were placed in appropriate stage holders, and examined by author SM with a JEOL JSM IT500HR field emission scanning electron microscope under variable pressure mode, and with attached EDS capabilities (Oxford Instrument X-Max 50 SDD with Aztec 3.3 software). 104 particles were analyzed with EDS collectively in 12 representative 450x SEM fields, across the two sample-containing stubs, along with control spectra from the blank carbon disc and the metallic underlying aluminum stub. Carbon discs with talc revealed particles generally in close juxtaposition. To simplify the elemental analysis, particles that were geographically isolatable from one another were selected for analysis. EDS analysis was done

under quantitative spot acquisition mode to analyze elemental compositions (atomic weight % ratios). The 104 particles selected for analysis were representative in appearance and size, with the small exception that any fibers identified (3:1 aspect ratio or greater, and approximately parallel sides) were selectively analyzed. Dead time was consistently under 10% and EDS signal counts were generally 3000–6000 per second. Pulse pile-up, window artifact, oxygen stoichiometry, and carbon deconvolution corrections were applied through the Aztec (Oxford Instruments, Lexington, MA) software for all EDS runs. Elemental data for all particle EDS analyses were then aggregated into a spreadsheet, and basic statistical parameters calculated. In compiling and analyzing all data, we started with the assumption that talc's Mg/Si ratio, like many parameters in medicine and science, has a normal (gaussian) probability distribution centered around a mean.

A separate sample of talc was obtained from Sigma-Aldrich (SA) (now known as Millipore Sigma, St. Louis, MO), Pcode 1001945014, lot# MKBS250TV. This sample of talc was characterized as ≤10 μm particle grade, and had been the main object of analysis in a previously published Raman spectroscopy study.[17] The SA talc was suspended in deionized water and sonicated on ice using multiple cycles with the Misonix XL-2000 sonicator (Misonix, Inc., Farmingdale, NY) to break up clumps and thus facilitate analysis. The SA talc sample was then filtered through a ~0.22μm Millipore filter and this was mounted onto a carbon disc with double-sided adhesive tape, and analyzed by author YF with a Hitachi SU6600 field emission scanning electron microscope with Oxford EDX (Xmax 50SDD EDX detector) and Oxford instrumentation software (Aztec 3.3). SEM/EDS analysis of SA talc proceeded in a similar way to that previously described for the JBP sample, including the use of spot quantitative acquisition mode on numerous representative particles, and the collection of elemental atomic weight % data collectively into a spreadsheet, with the subsequent calculation of basic statistical parameters. Also, the various aforementioned EDS corrective parameters and carbon deconvolution were employed here also.

Using the same Hitachi SEM instrument and its attached EDS capabilities, and spectral corrections, separate material from the aforementioned JBP bottle (the one analyzed by author SM) was analyzed, also by author YF, thus representing a third separate analytic study across the two different talc samples. The results were tabulated and compared to those obtained for the other two analyses (author YF for the SA talc sample, and author SM using the JEOL SEM on the JBP sample).

## Results

In the first part of the study, 104 particles from the JBP sample were representatively chosen and analyzed by author SM using SEM/EDS across 12 microscopic 450x SEM fields. A typical field showing the particle morphology is shown in Figure 1. In this figure, numerous backscattered-electron positive particles are seen, ranging in approximate size from 2–70 μm, showing varied geometric shapes, with polygonal particles and platy particles being common (as expected). Among the 104 characterized particles were 6 fibers; these showed talc molecular spectra similar to the far more numerous non-fibers. Overall, of the 104 particles, 99 showed magnesium, oxygen and silicon peaks only (along with the expected carbon background peak), in the molecular signature expected for talc (Figure 2). 50 of these particles had small aluminum peaks (atomic weight % consistently <2), which we regarded as a background signal coming from the instrument, and detected by EDS. In support of this contention, small aluminum peaks of similar height were detected by EDS in the blank (control) carbon discs, as well as in occasional areas of the sample-containing discs but in bare regions at a distance from talc particles. (Figure 3). These aluminum peaks were variably and irregularly present, but tended to be more noticeable at the periphery. Also, EDS of the bare aluminum stub (no carbon disc on top) produced a strong aluminum peak (as expected), along with a much smaller copper peak (Figure 3). The aluminum signal did not relate to the presence of adhesive on the carbon disc surface, since we tested disc regions both with and without adhesive (areas of denudation of the latter were visible and easily found), and this did not correlate with the

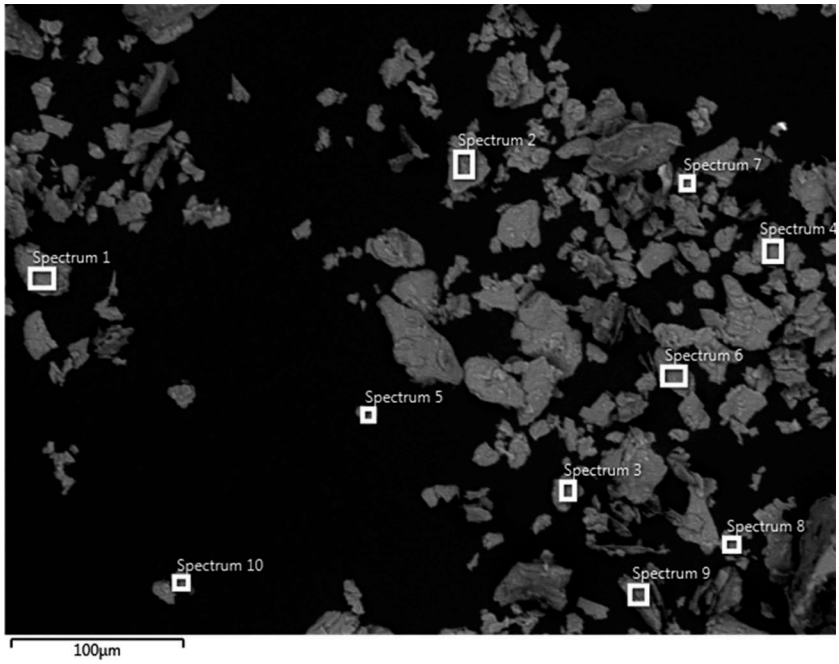


**Figure 1.** Representative SEM field for the JBP sample, under backscattered-electron imaging mode, showing particles widely varied in size and shape, generally 2–70 mm. (See size bar at lower left). Spectral boxes show particles representatively chosen for analysis by EDS under spot quantitative acquisition mode. Spectrum 1 was Mg-Al-Si (see Figure 4); the other particles were talc (Mg-Si). This represents one of many SEM fields that were examined (see text, main paper). (450x).

presence of Al peaks or any other unexpected signals.

Therefore, for the purposes of analysis, the aluminum signal was deconvoluted (using the Aztec software) from the 50 particles where this small signal had been seen. For all particles, carbon (C) had also been deconvoluted (see Materials and Methods section). Through this process, the extraneous peaks were numerically excluded from the spectrum, leaving accurate atomic weight % figures for the remaining elements (in this case, Mg, Si, and O), while still numerically taking into account their spectral peaks and their effect on other molecular signals (for example, overlapping peaks or peak slopes which are near other signals). Deconvolution using the Aztec EDS software typically produces slightly different numerical results than simple mathematical exclusion of elements in output results (also an option with the software), and was a more accurate way of eliminating certain elements from compositional calculations, particularly those regarded as background signals or contaminants, or otherwise not part of the intrinsic molecular structure of a given particle.

The remaining five particles out of the 104 were non-talc silicates. Four were Mg-Al-Si and one was K-Mg-Al-Si. Under SEM, these were morphologically not distinguishable from the talc particles. Their Mg/Si atomic weight % ratios differed significantly from those of the talc particles (even the latter's numerical outliers), with the Mg value typically close to Si (4 particles) or far smaller (one particle). Also, their aluminum peaks were much larger (>2% weight percent ratio by EDS) than the background contribution from the instrument when it happened to be seen in the talc particle spectra. Thus these five silicate particles were regarded as definitively not talc. An example of a Mg-Al-Si silicate is shown in Figure 4.

For the 99 talc particles which remained after the above exclusions were done, the Mg/Si atomic weight % mean for the 48 particles requiring aluminum deconvolution was very similar (0.634) to the 50 which did not (0.637). Therefore, the two groups were combined (for computational purposes), and the resulting Mg/Si atomic weight % ratio mean was 0.636 (range, 0.538–0.682) and the standard deviation was 0.026.

Using the same JBP sample in the Hitachi SEM, 96 particles were analyzed with EDS by YF. Some of them had small peaks for aluminum, and many had small peaks for iron. The latter is a frequent

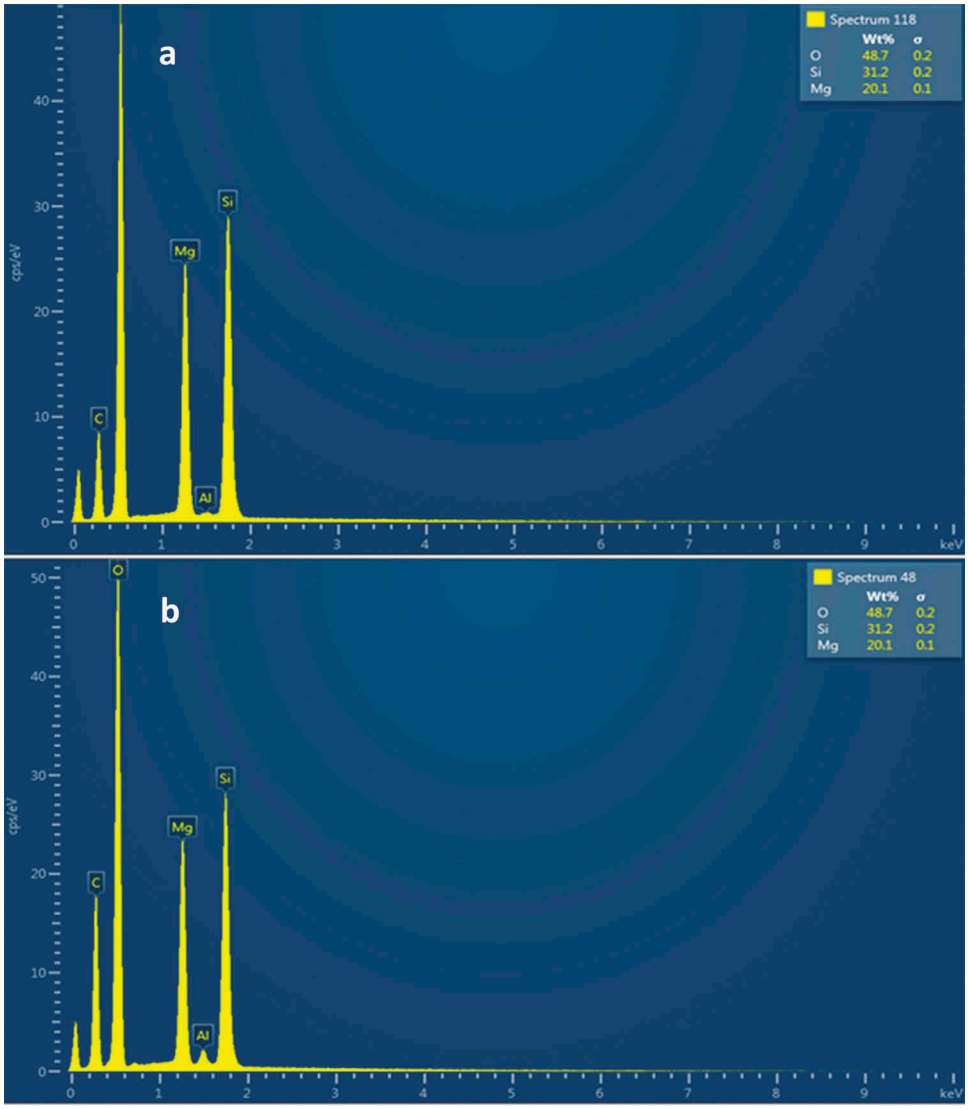


**Figure 2.** Representative spectrum of two talc particles from the JBP sample. Peaks for Mg and Si are present, along with a peak for O at approximately 5 keV. The Mg/Si atomic weight % ratio for both particles is 0.644 (see spectral data in upper right hand corner), which is typical for talc and is within 1% of the theoretical value of 0.649. (a) top spectrum: no background Al (aluminum) peak was detectable in this particle. (b) bottom spectrum: a small Al peak (atomic weight % <2) was seen here, as it was in about half the JBP particles we analyzed. These small Al peaks, when present, were thought to come from the EDS background environment, specifically the underlying metallic stub (see Figure 3; also see text, main paper). For particles otherwise having the characteristics of talc, these Al signals were deconvoluted prior to computations of data (see main paper for details).

impurity in talc where its II and III oxidation states may substitute for magnesium.[1] Four particles were regarded as non-talc silicates because they had an aluminum atomic weight % >2 (range, 6.04 to 10.49). One particle was excluded from the talc category because it had an iron atomic weight % >3 (exact value 3.64). Of the remaining 91 particles, the mean Mg/Si atomic weight % ratio was 0.638 (range, 0.547–0.682; standard deviation 0.028).

276 particles from the SA talc sample were analyzed with EDS by YF with the Hitachi SEM. 36 of these were silicates that were categorized as non-talc because they had an atomic weight % figure of >2% for Ca, Ti, or Al, or >3% for Fe. (We used a slightly higher threshold for iron compared with the other metals, since Fe is a particularly frequent low-level contaminant in talc; this seemed to be especially true in the SA sample that we analyzed). The overall distribution

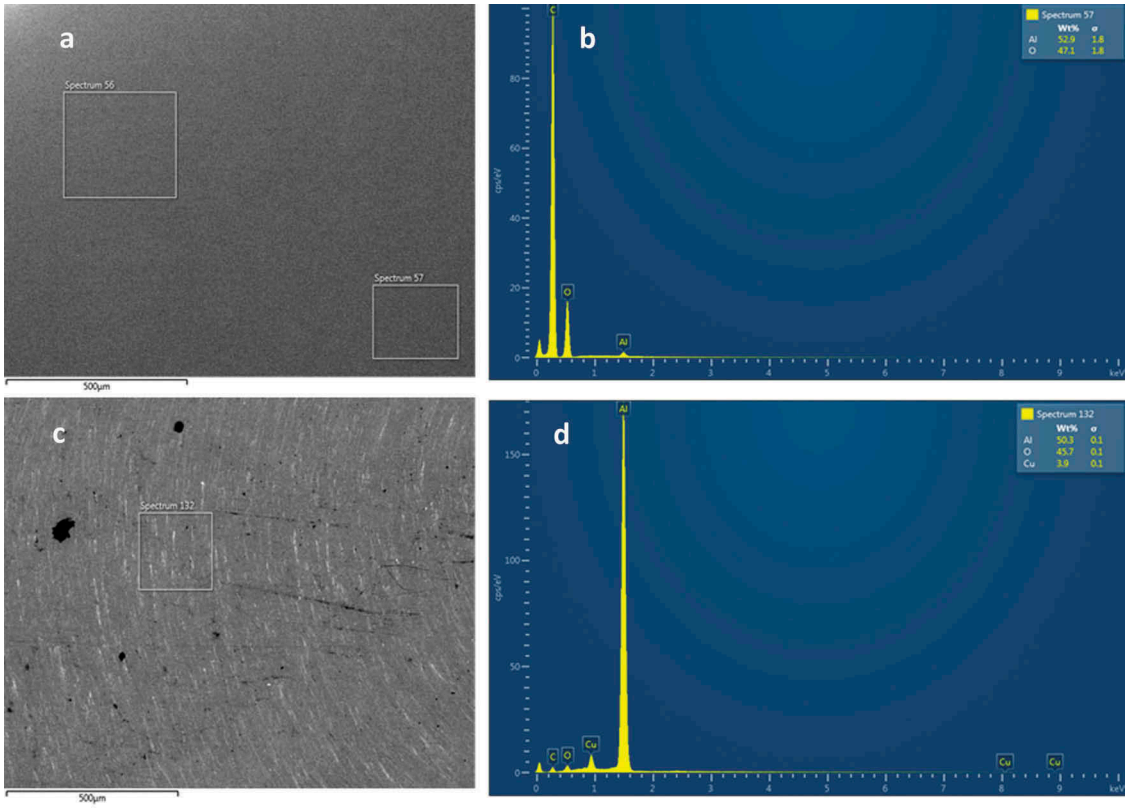


**Figure 3.** (a) Upper left: SEM view of blank adhesive carbon planchette, i.e. without talc sample, for control purposes. (b) upper right: EDS spectrum of surface in A showing small aluminum (Al) peak. This was variably present in the blank planchette – seen in some areas, not in others. (c) Lower left: SEM view of blank aluminum stub without planchette or sample. (d) Lower right: EDS spectrum of surface in C showing strong Al peak and weak Cu (copper) peak. Contribution of Al signal from the stub was thought to be the source of small Al peaks that were seen in some particle spectra (see text, main paper) and that were deconvoluted from such spectra prior to computational analysis. (a and c, 450x).

of these 36 silicates was: Mg-Al-Si (19), Mg-Fe-Al-Si (6), Mg-Ca-Si (4), Mg-Ti-Al-Si (3), Mg-Al-Ca-Si (2), Mg-S-Fe-Si (1), and Mg-Ti-Si (1).

In addition, a cluster of 29 consecutive Mg-Si-containing particles were excluded because their Mg/Si atomic weight % ratios (range 0.454–0.603) were most similar to sepiolite (0.576), although the morphologic features of these particles did not reveal the typical morphologic characteristics of sepiolite. Statistical comparison of this 29-particle cluster (Mg/Si atomic weight % ratios) to the remainder of the data showed F-test *P*-value ~ $10^{-4}$, and two-sample t-test *P*-value ~$10^{-15}$. Given their very different ratios from the rest, their appearance as a cluster, and the statistical calculations above, these sepiolite-like particles were excluded; 211 talc particles (Mg and Si-only peaks) remained. These had an Mg/Si atomic weight % ratio mean of 0.652 (range 0.501–0.711, standard deviation = 0.020).

When all 401 talc particles from the three branches of our study (JBP sample on the JEOL SEM and Hitachi SEM, and SA talc sample on the Hitachi SEM) were combined for computational analysis, the Mg/Si atomic weight % ratio mean was 0.645 (range, 0.501–0.711; standard deviation 0.025). Figure 5 shows a frequency distribution chart for the Mg/Si ratios for all talc particles in the study (n = 401). This shows that the data values conform closely to the pattern expected for a normal (gaussian) distribution. Table 1 summarizes the comparative statistics for the three main parts of our study (n = 99, 91, and 211, respectively), as well as the statistics for the combined particle data (n = 401). Our study analyzed a wide variety of small and larger talc particles across the samples and the two different microscopes, ranging from 1.2 to 66.9 µm. Table 1

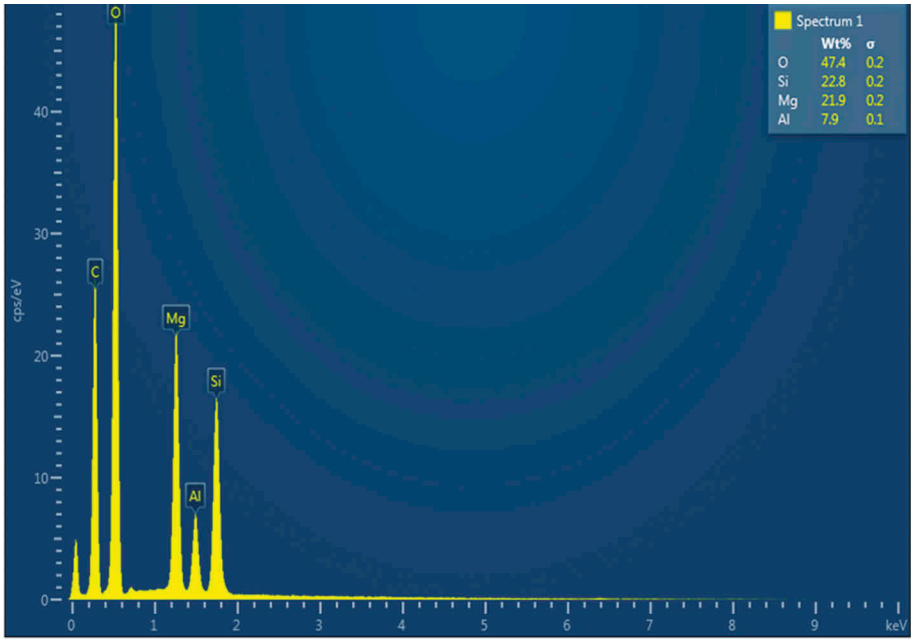


**Figure 4.** EDS spectrum for particle labeled as Spectrum 1 in Figure 1, from the JBP sample. This shows a magnesium aluminum silicate, with aluminum (Al) peak much stronger than the background Al signal seen in some talc spectra in this study (see Figure 2, and text of main paper). Also, the atomic weight % data (upper right) shows Mg about equal to Si, which is very different from that expected for talc. Thus the Al signal is regarded as an intrinsic part of the particle, and this represents a non-talc silicate. Such silicates accounted for about 5% of the total particles analyzed from the JBP sample.

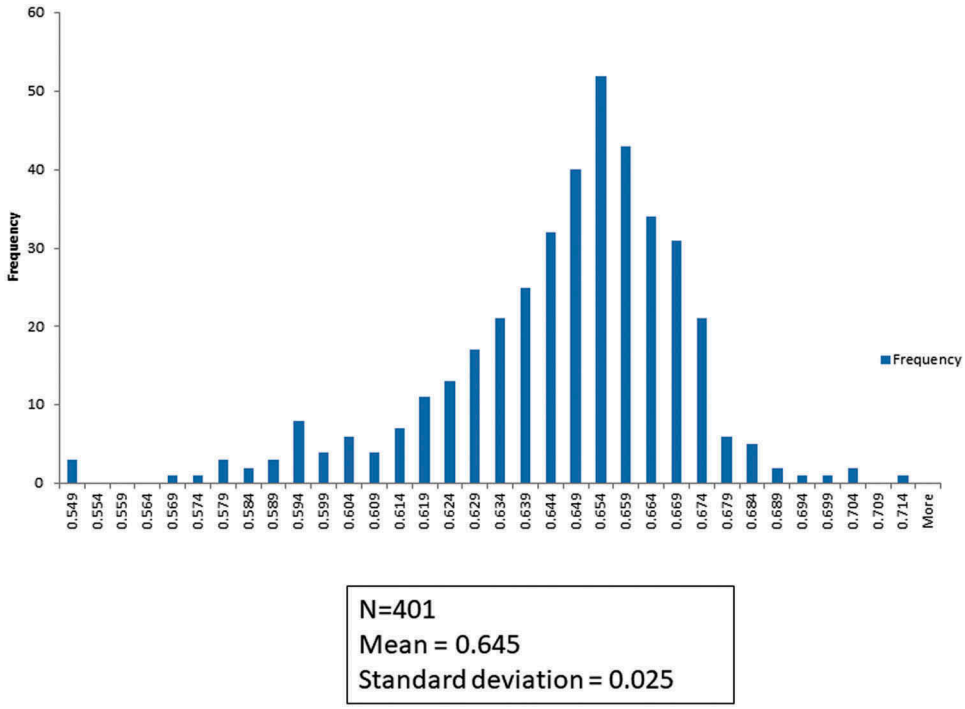


**Figure 5.** This figure shows the frequency distribution of Mg/Si atomic weight % ratios in the combined data for the JBP and SA talc samples.

**Table 1.** Comparative statistical parameters for the three different SEM/EDS talc analyses in our study.

| Sample Characteristics of sample | JBP sample, JEOL SEM analysis | JBP sample, Hitachi SEM analysis | SA talc sample, Hitachi SEM analysis | Combined data |
|---|---|---|---|---|
| *# talc particles analyzed* | 99 | 91 | 211 | 401 |
| *Mean particle size (greatest dimension listed in μm)* | 25.17 (standard deviation = 10.64) | 28.91 (standard deviation = 10.44) | 6.16 (standard deviation = 3.22) | 16.08 (standard deviation = 12.95) |
| *Mean Mg/Si atomic weight % ratio* | 0.636 (standard deviation = 0.026) | 0.638 (standard deviation = 0.028) | 0.652 (standard deviation = 0.020) | 0.645 (standard deviation = 0.025; ± 1σ = (0.620, 0.670) |
| *Maximum Mg/Si atomic weight % ratio* | 0.682 | 0.682 | 0.711 | 0.711 |
| *Minimum Mg/Si atomic weight % ratio* | 0.538 | 0.547 | 0.501 | 0.501 |

also shows the mean particle sizes in the different parts of the study.

## Discussion

The accurate identification of talc in human pelvic tissues, particularly those from ovarian cancer patients, is important because it documents exposure, and provides evidence in support of its epidemiological association with certain types of ovarian cancer that has been seen in various case control studies.[2–7] Typically, talc particles that lodge in human pelvic tissues are relatively small, with about 92% of 200 talc particles recently studied in surgically resected tissues from 11 ovarian carcinoma patients having a greatest dimension of ≤10 μm, though such particles ranged up to 29 μm.[23] The common sizes of talc particles found within human pelvic tissues[10] overlaps with, but is typically smaller than, the particle size range found in talc powder material intended for consumer sale and hygienic use.[23] The likely reason is that smaller talc particles are the ones thought most able to gain access to reproductive tract space, or especially into small submucosal lymphatics, when applied to the perineum.[10] An earlier study on cynomolgus monkeys had cast doubt on the ability of talc to migrate in this way[24]; however no talc particle size data was presented, and without that data, a meaningful comparison with the subsequent human literature is difficult or impossible. Studies show that small particle-sized radiographic tracers easily traverse the lymphatic vessels of the female genital tract[25–27], and the lymphatic network of this area is considerably more extensive than is often appreciated.[28,29]

Generally, our analyses of two different commercial talc samples (JBP and SA talc), with two different SEM/EDS systems, support the currently used criterion in medical/medicolegal settings of a ± 5% range for the Mg/Si atomic weight % ratio (corresponding to 0.617–0.681 based on the theoretical 0.649 ratio) in the definitive diagnosis of talc, for particles that are morphologically and spectrally consistent with talc. Our combined analyses (401 talc particles overall) showed a mean Mg/Si atomic weight % ratio of 0.645, very close to the theoretical value of 0.649. The overall standard deviation was 0.025, with ± 1σ (~68% of all particles) = 0.620–0.670, and ± 2 σ (~95% of all particles) = 0.595–0.695. The latter range is conceptually significant because a 95% confidence interval is regarded as an important threshold in human medicine, whereby values or data points which fall outside this range are regarded as suspect, or possibly due to something other than chance or random variation. This is the reason why it is used frequently as a reference interval for laboratory values which assume a normal (gaussian) probability distribution.[30] Because the currently used ± 5% range criterion is between the ± 1σ and ± 2σ ranges in our analytic study, but closer to ± 1σ, the ± 5% criterion is more conservative than a standard 95% confidence interval (i.e. ± 2σ) would be. Given that it is currently being applied in medicolegal contexts involving tissues from exposed patients, this conservative approach is appropriate and so its continued use seems justified. An inclusion range based on standard deviation around a mean is much better than one based on simply the mean, since the standard deviation captures the degree of variation present in talc, and so helps inform what an appropriate standard for inclusion should be.

Like many parameters in chemistry, the Mg/Si talc atomic weight % ratio is subject to natural variation across samples. As an example of a literature

precedent, ranges of elemental compositional ratios have been demonstrated in vermiculite using EDS, and graphed using a two-dimensional dot plot.[31] For talc, Mg/Si ratio variances can occur from the composition of talc itself, or factors (previously discussed in the Introduction section) in the spectroscopic method.

As an example of the former, although Figure 5 conforms reasonably closely to a gaussian distribution, the slope on the left side (lower Mg/Si atomic weight % ratios) is somewhat more gradual, and extends further out, than the one on the right side (higher ratios). This is likely reflective of the greater lability of magnesium in talc relative to silicon; Mg-O bonds are more easily broken and/or affected by dissolution reactions than are Si-O bonds[32]; thus over time the content of Mg relative to Si in talc could decrease gradually and variably, especially for areas near the particle surface.[32] Another factor is that impurities are common in talc, whereby certain elements, such as aluminum, iron and titanium, may substitute for magnesium and/or silicon.[1]

Regarding chemical variations, talc deposits in the earth may be accompanied by many other minerals, and this varies significantly by geography. Some of these include magnesite, $MgCO_3$, and quartz, $SiO._2$[1] If present, the former would contribute magnesium atoms and not silicon, whereas the reverse is true for quartz. Also, there are minerals that, similar to talc, show EDS peaks for Mg and Si without other elements with atomic number >10, that need to be distinguished from talc. Morphology is key in this distinction, but the Mg/Si ratio also plays a key role. For example, chrysotile asbestos is a magnesium silicate but unlike talc, is virtually always fibrous (except in rare instances where small pieces of a fiber might dislodge and assume a non-fibrous particle appearance). The Mg/Si atomic weight % ratio for chrysotile is 1.298[14], and this is very different from talc, falling far outside the ± 2σ range for the latter's Mg/Si ratio. Anthophyllite, a noncommercial amphibole asbestos fiber type, normally has an iron peak along with Mg and Si, but its atomic structure may vary, and in a situation with low iron content, only Mg and Si peaks would show and the Mg/Si atomic weight % ratio would be 0.757. This is different from talc, and measurement of this ratio along with observation of fibrous structure would help with differentiation. Other asbestos subtypes have other cations with Mg and Si and so produce spectra that should not be confused with talc.

Regarding nonasbestos Mg-Si materials that enter into the spectral differential with talc, there is sepiolite, a common industrial material with formula $Mg_4Si_6O_{15}(OH)_2{\cdot}6H_2O$, having Mg/Si atomic weight % ratio 0.576 (again, distinct from talc, though closer to it than some other materials). If a ± 2σ range were used to identify talc, it is likely that the range for sepiolite would overlap. Importantly, sepiolite has a loosely fibrillar appearance (consisting of very small fibers) whose morphology is quite different from that of talc. Other Mg-Si materials to be considered are enstatite ($MgSiO_3$, Mg/Si atomic weight % ratio 0.865) and fosterite ($Mg_2SiO_4$, Mg/Si atomic weight % ratio 1.731). In our experience, these would be rarely encountered, and their Mg/Si spectral ratios would readily provide differentiation from talc. Thus, the use of ±5% of the theoretical atomic weight percent ratio for the identification of talc, although less than a ± 2σ or 95% confidence interval based on the analysis of standard materials, maximizes the 'true positive' identification of talc particles and limits the possibility of false positive identification of other magnesium silicates as talc.

Our study was significant in showing nonfibrous, non-talc silicates (Mg-Al-Si, K-Al-Mg-Si, and Fe-Mg-Si) as a component of the JBP sample (10/190 particles, or 5%, with the most common being Mg-Al-Si (8 particles, 4%). Given the tightly controlled and sealed conditions under which our JBP bottle was stored and used, these silicates are likely not laboratory contaminants, but rather may represent impurities in the sample that come from the talc mining and/or manufacturing process. Incidentally, various non-talc silicates may commonly be seen in the genital tract and pelvic tissues of human patients, whether talc-exposed or not[10]; such particles are generally regarded as nontoxic at the levels typically encountered, and are thought to enter the genital tract through various hygiene practices and daily living. Regarding the JBP sample, talc powder available to consumers for hygienic use would fall into the commercial classification known as 'cosmetic talc' which has >98% talc, possibly lower in older samples[8,33,34]; thus impurities of a few percent in a relatively small study such as ours are compatible with this

classification. Non-talc silicates were also found in the SA talc sample, in a higher proportion than for the JBP sample: 36/277 particles (13.0%) fell in this category, perhaps reflecting the different classification grade of this sample relative to JBP.

Also significantly, we found fibrous talc particles in our samples. In the JBP sample analyzed on the JEOL SEM, 6/99 EDS-analyzed talc particles (6%) had this morphology. For the JBP sample analyzed on the Hitachi, 0/91 such particles (0%) were fibers, and for the SA talc sample on the Hitachi, 10/211 (5%) were. Figure 6 shows an example of a talc fiber with an approximately 4.8:1 aspect ratio that was found in the JBP sample, with an Mg/Si atomic weight % ratio of 0.650. IARC lists talc containing asbestiform fibers (defined by IARC as talc forming mineral fibers that are asbestiform in their mineral "habit", *not* talc containing asbestos) as a class I carcinogen.[8] The reader is referred to the literature for a mineralogic discussion of the term asbestiform as it relates to silicates.[35] The proportion of talc asbestiform fibers overall in these samples is likely substantially lower than the percentage figures cited above, since we selectively analyzed fibers by EDS when we saw them in our representative microscopic fields. Fibrous particles (talc or otherwise) are important, because the Stanton hypothesis[36] stipulates that longer fibrous particles may have greater capacity for cellular damage than comparable shorter fibers or non-fibrous particles of similar size and composition. Although particulate material with a plate-like morphology such as talc can mimic fibers if turned on edge, this is more likely within tissue than in a material sample such as used here. However, our results mirror what we have observed in talc-exposed human patients, namely that fibrous talc (and fibers in general) account for a small proportion of the overall particle burden in the pelvic tissues of such patients.[10]

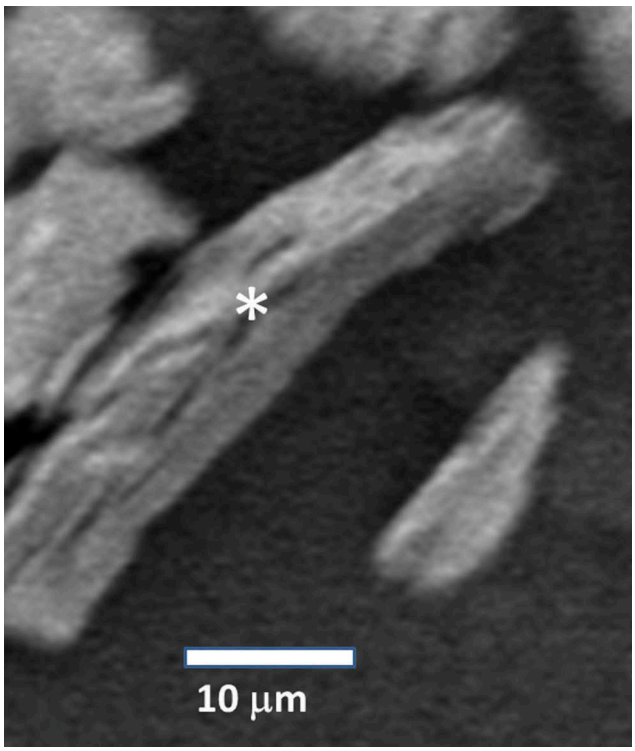


**Figure 6.** Asterisk (*) shows a talc fiber with approximately 4.8:1 aspect ratio and parallel sides. By EDS, this particle showed a spectrum for talc very similar to those in Figure 2, and the Mg/Si atomic weight % ratio was 0.650, very close to the theoretical ratio for talc (0.649). As explained in the main text, fibrous talc particles were uncommonly encountered in the samples we examined. (SEM, original magnification 450x).

In conclusion, our study supports the continued use of a 0.649 ± 5% range for the Mg/Si atomic weight % ratio for the diagnosis of talc in human tissue in medical/medicolegal settings. Our study also reinforces the concept that for SEM/EDS in elemental compositional assessments, it is important to do the proper controls, and take into account the possibility of background peaks arising from the analysis or SEM environment and not from the sample itself.

## Acknowledgments

The authors acknowledge Mr. Ben Karasko for his assistance with morphology measurements in this study.

## Declaration of interest statement

The authors declare the following competing financial interest(s): JJG has served as consultant and provided expert testimony in talc and other environmental litigation. SM, YF, and RR report no conflicts of interest.

## Funding

Funding for this research was provided through John J. Godleski, MD PLLC.

## References


1. IARC (International Agency for Research on Cancer). *Monograph 93-8C., IARC Working Group on the Evaluation of Carcinogenic Risks to Humans*, Lyon, France; 2010:277–413. doi:10.1603/ec09292.
2. Cramer DW, Welch WR, Scully RE, Wojciechowski CA. Ovarian cancer and talc. *Cancer*. 1982;50:372–376. doi:10.1002/1097-0142(19820715)50:2<372::AID-CNCR2820500235>3.0.CO;2-S.
3. Cramer DW, Lieberman RF, Ernstoff LT, et al. Genital talc exposure and risk of ovarian cancer. *Int J Cancer*. 1999;81:351–356. doi:10.1002/(SICI)1097-0215-(19990505)81:3<351::AID-IJC7>3.0.CO;2-M.
4. Cramer DW, Vitonis AF, Terry KL, Welch WR, Titus LJ. The association between talc use and ovarian cancer: a retrospective case-control study in two US states. *Epidemiol*. 2016;27:334–346. doi:10.1097/EDE.0000000000000434.
5. Schildkraut JM, Abbott SE, Alberg AJ, et al. Association between body powder use and ovarian cancer: the African-American Cancer Epidemiology Study ((AACES). *Cancer Epidemiol Biomarkers Prev*. 2016;25:1411–1417. doi:10.1158/1055-9965.EPI-15-1281.
6. Terry KL, Karageorgi S, Shvetsov YB, et al. Genital powder use and risk of ovarian cancer: a pooled analysis of 8,525 cases and 9,859 controls. *Cancer Prev Res*. 2013;6:811–821. doi:10.1158/1940-6207.CAPR-13-0037.
7. Penninkalimpi R, Eslick GD. Perineal talc use and ovarian cancer: a systematic review and meta-analysis. *Epidemiol*. 2018;29:41–49. doi:10.1097/EDE.0000000000000745.
8. IARC (International Agency for Research on Cancer). *Volume 100C, IARC Working Group on the Evaluation of Carcinogenic Risks to Humans*. Lyon, France: World Health Organization; 2012:1–501.
9. McDonald SA, Fan Y, Welch WR, et al. Correlative polarizing light and scanning electron microscopy for the assessment of talc in pelvic lymph nodes. *Ultrastruct Pathol*. 2019;43:13–27. doi:10.1080/01913123.2019.1593271.
10. McDonald SA, Fan Y, Welch WR, Cramer DW, Godleski JJ. Migration of talc from the perineum to multiple pelvic organ sites: five case studies with correlative light and scanning electron microscopy. *Am J Clin Pathol*. 2019;152:590–607. doi:10.1093/ajcp/aqz080.
11. Cramer DW, Welch WR, Berkowitz RS, et al. Presence of talc in pelvic lymph nodes of a woman with ovarian cancer and long-term genital exposure to cosmetic talc. *Obstet Gynecol*. 2007;110:498–501. doi:10.1097/01.AOG.0000262902.80861.a0.
12. Abraham JL. Analysis of fibrous and nonfibrous particles. In: Rom WN, Markowitz SB, eds. *Environmental and Occupational Medicine*. 4th ed. Philadelphia: Lippincott Williams and Wilkins; 2006:277–297.
13. Roggli VL. Asbestos bodies and nonasbestos ferruginous bodies. In: Roggli VL, Greenberg SD, Pratt PC, eds. *Pathology of Asbestos-Associated Diseases*. Boston: Little Brown; 1992:39–75.
14. McDonald JW, Roggli VL, Churg A, et al. Microprobe analysis in pulmonary pathology. In Ingram P, Shelburne JD, Roggli VL, et al. eds. *Biomedical Applications of Microprobe Analysis*. San Diego: Academic Press; 1999:201–256.
15. Thakral C, Abraham JL. Automated scanning electron microscopy and x-ray microanalysis for in situ quantification of gadolinium deposits in skin. *J Electron Microsc*. 2007;56:181–187. doi:10.1093/jmicro/dfm020.
16. Electron beam-specimen interactions: interaction volume. Secondary electrons. X-rays. In: Goldstein JI, Newbury DE, Michael JR et al., eds. *Scanning Electron Microscopy and X-Ray Microanalysis*. Chapter 1, 3, 4, 4th ed. New York: Springer; 2018:1–14, 29–38, 39–64.
17. Campion A, Smith KJ, Fedulov AV. et al. Identification of foreign particles in human tissues using Raman microscopy. *Anal Chem*. 2018;90:8362–8369. doi:10.1021/acs.analchem.8b00271.
18. Vu VT. Health hazard assessment of nonasbestos fibers. Health and Environmental Review Division, U. E. Environmental Protection Agency, National Service Center for Environmental Publications. December 30, 1988. https://nepis.epa.gov/Exe/ZyNET.exe/91013R9A.TXT. Accessed October 11, 2019.
19. Backscattered electrons. In: Goldstein JI, Newbury DE, Michael JR et al., eds. *Scanning Electron Microscopy and X-Ray Microanalysis*. Chapter 2, 4th ed. New York: Springer; 2018:16–28.
20. Scanning electron microscopy and associated techniques: overview. In: Goldstein JI, Newbury DE, Michael JR et al., eds. *Scanning Electron Microscopy and X-Ray Microanalysis*. 4th ed. New York: Springer; 2018:VII–XIV.
21. Czyzewski Z, Joy DC. Fast Monte Carlo method for simulating electron scattering in solids. *J Microsc*. 1989;156:285–291. doi:10.1111/jmi.1989.156.issue-3.
22. Adesida I, Karapiperis L. Monte Carlo simulation of ion beam penetration in solids. *Radiat Effects*. 1982;61:223–233. doi:10.1080/00337578208229936.
23. Johnson KE, Popratiloff A, Fan YF et al. *Analytic Comparison of Talc in Commercially Available Baby Powder and in Pelvic Tissues Resected from Ovarian Carcinoma Patients* [Manuscript in preparation].
24. Wehner AP, Weller RE. On talc, translocation from the vagina to the oviducts and beyond. *Food Chem Toxicol*. 1986;24:329–338. doi:10.1016/0278-6915(86)90011-6.
25. Vanneuville G, Mestas D, Le Bouedec G, et al. The lymphatic drainage of the human ovary in vivo investigated by isotopic lymphography before and after the menopause. *Surg Radiol Anat*. 1991;13:221–226. doi:10.1007/BF01627990.
26. Nune SK, Gunda P, Majeti BK, Thallapally PK, Forrest ML. Advances in lymphatic imaging and drug delivery. *Adv Drug Deliv Rev*. 2011;63:876–885. doi:10.1016/j.addr.2011.05.020.
27. Darin MC, Gomez-Hidalgo NR, Westin SN, et al. Role of indocyanine green in sentinel node mapping in gynecologic cancer: is fluorescence imaging the new

standard? *J Minim Invasive Gynecol*. 2016;23:186–193. doi:10.1016/j.jmig.2015.10.011.

28. Varga I, Kachlik D, Ziskova M, Miko M. Lymphatic lacunae of the mucosal folds of human uterine tubes – a rediscovery of forgotten structures and their possible role in reproduction. *Ann Anat*. 2018;219:121–128. doi:10.1016/j.aanat.2018.06.005.
29. Geppert B, Lonnerfors C, Bollino M, Arechvo A, Persson J. A study on uterine lymphatic anatomy for standardization of pelvic sentinel lymph node detection in endometrial cancer. *Gynecol Oncol*. 2017;145:256–261. doi:10.1016/j.ygyno.2017.02.018.
30. Winkel P, Statland BE. Interpreting laboratory results: reference values and decision making. In: Henry JB, ed. *Clinical and Diagnosis Management by Laboratory Methods*. 18th ed. Philadelphia: WB Saunders; 1991:49–67.
31. Wright RS, Abraham JL, Harber P, et al. Fatal asbestosis 50 years after brief high intensity exposure in a vermiculite expansion plant. *Am J Respir Crit Care Med*. 2002;165:1145–1149. doi:10.1164/ajrccm.165.8.2110034.
32. Jurinski JB, Rimstidt JD. Biodurability of talc. *Am Mineralologist*. 2001;86:392–399. doi:10.2138/am-2001-0402.
33. Rohl AN, Langer AM, Selikoff IJ, et al. Consumer talcums and powders: mineral and chemical characterization. *J Toxicol Environ Health*. 1976;2:255–284. doi:10.1080/15287397609529432.
34. Zazenski R, Ashton WH, Briggs D, et al. Talc: occurrence, characterization, and consumer applications. *Regul Toxicol Pharmacol*. 1995;21:218–219. doi:10.1006/rtph.1995.1032.
35. Virta RL. Some facts about asbestos. US Geological Survey. 2001. https://www.luc.edu/media/lucedu/environmentalservices/images/facilities/asbestos_fact_sheet_usgs.pdf. Accessed October 18, 2019.
36. Boulanger G, Andujar P, Pairon J, et al. Quantification of short and long asbestos fibers to assess asbestos exposure: a review of fiber size toxicity. *Environ Health*. 2014;13:59. doi:10.1186/1476-069X-13-59.